January 2020

Full-scale propulsion measurements on a planing pleasure yacht in head sea

Riccardo PIGAZZINI [a,1], Fabio DE LUCA [b] Flavio BALSAMO [b] and Amedeo MIGALI [c]

[a] *Università degli Studi di Trieste*
[b] *Università degli Studi di Napoli "Federico II"*
[c] *MICAD s.r.l.*

Abstract. Full scale seakeeping trials are rare, especially planing hull and are in general focused in studying bottom pressures, accelerations and vibrations. In this paper, a comprehensive description of the experimental setup and analysis of full scale seakeeping trials propulsion data of a 65 ft planing pleasure yacht is presented. Torque and rpm have been measured on both propeller shafts during seakeeping trials in mild sea conditions, along with hull motions and accelerations. Correlations between hull motions and propulsion data are discussed, both in the time and frequency domain. Further tests on a shaft sample have been carried out in order to validate its mechanical properties and hence quantitative results regarding shaft torque. The main novelty of the present work lays in a detailed analysis of the propulsion system response of a planing pleasure yacht in mild weather conditions.

Keywords. Full-scale, propulsion, planing yacht, seakeeping

1. Introduction

The study presented in this work is part of the project SOPHYA (Seakeeping Of Planing Hull YAchts), co-funded by EU through the Regional Administration of Friuli-Venezia Giulia Region (Italy) POR FESR 2014-2020. The project focusses on the investigation of the performances of planing pleasure boats in terms of sea-kindliness, safety and powering in mild weather conditions. The study is pursued via three complementary approaches: sea trials, model scale experiments and CFD simulations. In this work, the full scale powering measurement are discussed. The sea trials were conducted on a 65 foot yacht built by Monte Carlo Yachts (http://www.montecarloyachts.it).

[1]Corresponding Author: Riccardo Pigazzini, Università degli Studi di Trieste, Via Alfonso Valerio, 6/1, 34127 Trieste (Italy); E-mail: riccardo.pigazzini@phd.units.it

1.1. Literature Review

One of the first and most known study on full scale data of planing hulls in waves is the work published by Allen and Jones [1]. They measured pressure, strain and accelerations on different high speed vessels in waves, two of which were conventional planing hulls. The aim of the study was to develop a simplified model for predicting the hull bottom impact pressure and provide boat designers an equivalent uniform static pressure for the scantling of hull structural components.

Kallio [2] compared the motions and accelerations recorded during Seakeeping trials on a ram wing planing craft and a conventional planing craft. The conventional planing hull was tested in head, bow and stern quartering and following sea at speeds up to 60 knots. The mostly unidirectional sea state had 0.7 m significant wave height. Significant double amplitudes of motions and accelerations were measured using a stabilized platform and accelerometer respectively. The seastate was recorded by means of a USCG wave buoy.

Ooms [3] carried out full scale data from two similar fast rescue vessels. The accelerations and motions measurements on both ships were carried out simultaneously. The focus of the work was to compare RMS and peak values of accelerations in the wheelhouse and bow sections of both hulls. All the measurements, including pitch, speed and course were sampled at 30Hz and analized using 10Hz lowpass filter. The tests were carried out at speeds ranging from 12 to 30 knots, the helmsman was not allowed to change route and/or speed. In the real world, this is not the case, see [13,14], but the full scale tests were designed to be as close as possible to the towing tank tests.

Akers [4] performed sea trials with a planing hull with the aim of validate the results obtained with a planing hull simulator. The tests were conducted with a 25-foot commercial utility boat. Accelerations and motions were measured using two three-axis accelerometers and a inertial measurement unit (IMU). The tests were carried out in calm water and in the wake generated by a passing boat. In addition to acceleration and motions, both wave and wake of the wavemaking boat were measured using wavebuoy and videocamera respectively. A summary of the maxima and minima of pitch and vertical acceleration are given in tabular form along with some timeseries plots of the same variables on selected runs.

Garme and Rosén [5] presented full-scale trials results of a swedish marine medical evacuation high speed craft. The study was focused on the characteristics of slamming impacts and the validation of the proposed numerical method. The Storebro SB90E used in the tests was 9.5 m long, had a displacement of 6.5 tonnes and speeds varying from 10 to 40 knots. They measured motions with a 15Hz Inertial measurement unit (IMU)and vertical accelerations with 2kHz accelerometers. The craft was also equipped with 2kHz pressure transducers, shear and strain gauges in order to record pressure peaks and structural response. Although the high sampling rate, it was found that it was sometimes too low to capture pressure peaks. The sea trials were performed in head ($\chi = 180°$) and bow sea ($\chi = 150°$)conditions and speeds ranging from 10 to 40 knots. Interestingly, it has been found that in bow seas presents higher impact pressure and lower impact acceleration respect to head seas.

Mørch and Hermundstad [6] presented results of accelerations, pressures, strain and deflection measurements on a planing pleasure craft in waves. The aim of the study was to gain a better understanding of slamming loads and structural response of a planing craft at sea. The Nidelv 610 craft used in the sea trials is 6.1 m long and has a displacement of 1550 Kg. Sea state was measured by a single accelerometer on a PVC float, where all on-board measurements were sampled at 750 Hz and filtered through moving average. It was found that although a large safety margin is used in the DNV rules, design pressures were easily exceeded during tests.

Keuning [7] published the results of an extensive research program on three 55 meter long monohull Patrol Boat concepts. The aim of the study was to gain insight on the aspects that most impact the craft operability at sea and try to evaluate their limit values of motions and accelerations in order to ensure safe operation of the ship. Hull design was the main variable explored in the research in order to evaluate three radically different bow geometries. The tested ships motion and accelerations were recorded during a large number of runs while performing their usual tasks under real circumstances at sea. Other than the usual sea state and motion measurements, the throttle position has been recorded in order to detect voluntary crew speed reductions.

Townsend [8] performed full scale sekeeping tests on a Royal National Lifeboat Institution (RNLI) Atlantic 75 rigid inflatable boat (RIB) in order to study the influence of speed, ballast, wave height, encounter frequency, and tube pressure on RIB motions.

Recently, Prini et al. [10] published the results of full scale tests on a RNLI Severn class all-weather lifeboat. Strain gauges, accelerometers and rate gyros have been used to sample structural strain, accelerations and rigid motion. Accelerations and strain, subject to sudden variations, were sampled at 2048Hz, rigid body motions at 256 Hz. The sea state was measured by a Datawell GPS wave buoy. Results of the tests were analysed both in time domain using statistical indicators and in frequency domain in order to compute Response Amplitude Operators of the vertical bending moment. Results were compared with the results from a marine structural analysis software.

Camilleri et al. [11] carried out Full-scale trials on a 9.6m high-speed marine target autonomous planing craft. The aim of the tests was to investigate the characteristics of slamming impacts and its effect on motions and structural response. An extensive set of experimental data on accelerations, pressure and strain of the hull at sea has been presented. Accelerations and strain have been measured at the helm and bow, water pressure in more than 20 places on the hull and global hull deflections were measured using linear position sensors. The pressure peaks are fitted to Weibull and Generalized Pareto statistical models using a least squares parameter identification technique. A strong correlation between pressure and structural strain is observed, and larger values have been recorded at high speed in moderate seas instead of at moderate speed in high sea states. It is also found that ISO standards and DNV rules underpredict slamming pressure, LR rules instaed overestimate it although being closer to the observed values.

2. Experimental Setup

The sea trials that took place in the Gulf of Trieste (North Adriatic Sea) during the period December 2017 - January 2018. The experimental campaign took a total of four days of tests. Sea trials were carried out both in calm seas and in waves.

The duration of each run is around 10 min, which leads to a covered distance of 3 nm at 18 kn. Along this distance, the sea state is assumed reasonably homogeneous. Wind waves only (no swell) were present in the sea-trial area. It can be noted from Table 1 that the zero-crossing period (derived from the frequency-domain analysis of the free surface elevation) is generally very small, according to the geographic area and the target wind conditions. In particular *Run* 1, 4 and 5 are considered as limit conditions for the proper use of the buoy. Indeed for these specific records, log files from the wave buoy showed a non negligible number of errors. Still H_s met the project targets fairly well.

During the tests, the hull had no interceptors and trim flaps were kept in fully raised position. The design boat speed for the sea trials was 18 kn. Since a speed control system was not available, the tests were conducted at prescribed engine rpm and consequently the vessel speed varied slighty during the runs due to the waves. In table 1 the standard deviation of the vessel speed is reported. Fig. 1 shows an example of speed and course time series.

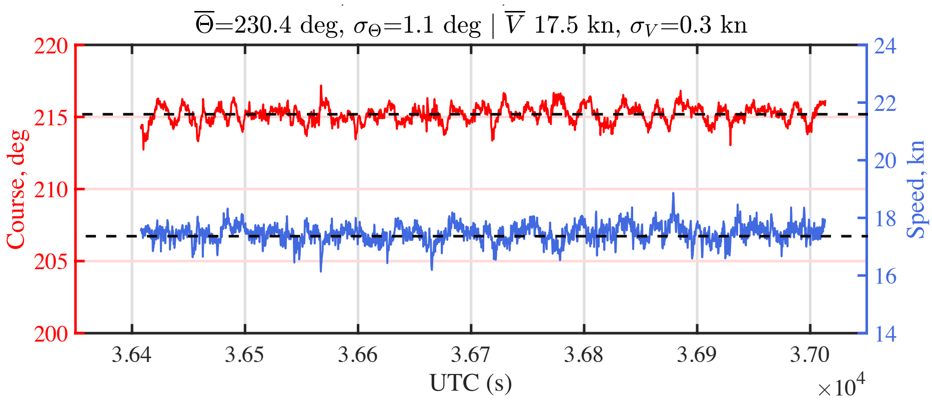

Figure 1. Sample time series of ship speed and course. $\overline{\Theta}$: Mean boat direction, σ_Θ: Boat direction standard deviation, $\overline{V}$: Mean boat speed, σ_V: Boat speed standard deviation

In accordance with the project targets, head sea conditions only were tested and analyzed. For every run, the target vessel heading was identified from the analysis of the last record available from a dedicated in-situ directional wave buoy. The target sea state of the project is here defined as *mild weather conditions* corresponding to a significant wave height H_s of about 0.50-0.60 m. These are very low sea state conditions that may take the measurement system (buoy) to its intrinsic lower limits, in particular in the presence of short-crested sea.

	date (dd/mm/yyyy)	time (hh:mm:ss)	H_s (cm)	T_z (s)	V (kn)	σ_V (kn)
Run 1	15/12/2017	13:02-13:13	60	3.1	18.4	0.4
Run 2	16/01/2018	14:17-14:25	59	4.8	17.4	0.3
Run 3	16/01/2018	14:47-15:57	60	4.8	18.5	0.4
Run 4	18/01/2018	10:06-10:16	54	3.5	17.5	0.3
Run 5	18/01/2018	11:09-11:18	43	3.0	18.6	0.4

Table 1. Sea state and average boat speed during the tests. H_s: Significant wave height, T_z: Wave period (zero-cross)

2.1. Sea State Measurements

A directional Datawell Waverider DWR-G4 buoy (diameter = 0.4 m, weight = 170 N), moored in the sea-trial area, was used as main source of wave information. The GPS technology supersedes the need for calibration of accelerometer and compass based sensors and it is not affected by spinning or manual handling. One potential disadvantage is that wave wash on the GPS antenna or extreme tilting could mask the signal. This only happened sporadically and for a few seconds during the whole deployment time. As a 30 min logging windows of the time series were considered, signal masking did not represent an issue.

Wave properties expressed in directional spectral form are given as energy and mean wave direction for each frequency f_i, with $i = 1, \ldots, N_f$. Actual encounter spectra are then derived using the integrated analysis of the sea state and on-board data presented in [9].

2.2. Loading condition measurements

The yacht loading condition is assessed every test day. Three depth measurements are carried out by hand. The measured depths and distance will be used to define the actual waterplane and then the loading condition parameters computed computed using Orca3D plugin.

2.3. Ship Motions Measurements

The onboard measuring system for ship motions consisted in 3 Xsens Inertial Measurement Units (IMU) and additional Global Navigation Satellite System (GNSS). A sensor fusion algorithm uses the data from all the sensor in order to reduce noise and improve accuracy in the output of the orientation data. In particular, IMU1 and IMU2 are Xsens MTi-G-700 have an extra SMA connector to allow a 72 channel GNSS receiver (GPS, GLONASS, BeiDou and Galileo) antenna to be attached, this allows for additional synchronized position and speed tracking during the sea trials.

Orientation, gyro and acceleration data from the IMUs are computed using the sensor-fixed output coordinate system. In order to be have correct roll, pitch and yaw readings, IMU1 has been carefully placed in the CG of the yacht, making sure that the sensor-fixed X axes is aligned to the yacht centerline. The GNSS reciever of IMU1 was taped to the master bedroom portside porthole, the one connected to the IMU2 to the starboard porthole in order to ensure the best satellite coverage possible.

IMU2 was placed at the same longitudinal position of CG but at starboard and IMU3 in the middle of the bow cabin (see Fig.2 for the layout).

The proprietary acquisition system of the IMU samples accelerations, rate of turn and compute Euler angles at 100 Hz whereas GNSS data are sampled at 4 Hz. The sensor fusion algorithm uses acceleration, magnetic and gyro data to interpolate latitude,longitude, speed and course data between two consecutive GNSS fix.

The logging frequency is 100Hz for all three IMUs, after being processed by the sensor fusion algorithm (IMU1 and IMU2) or Kalman filter (IMU3).

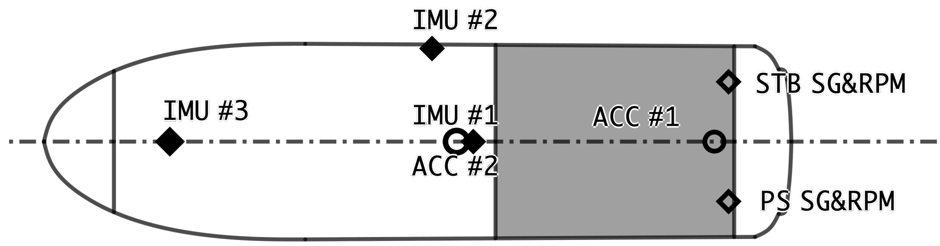

Figure 2. Onboard measuring systems layout

2.4. Ship Propulsion System Measurements

During the sea trials, one of the project goal was to not only monitor and log attitude and motion of the yacht but also the propulsion characteristics. The measure or monitoring of the propulsion onboard ships is carried out by measuring the torsional deformation and rotational speed of the propeller shaft. Once the deformation is assessed, shaft torque is computed using the shaft's mechanical properties, in particular, its shear modulus G (N/m^2):

$$G = \frac{E}{2(1+\nu)} \tag{1}$$

Where E is the Young's modulus and ν is the Poisson's ratio. For a circular shaft subjected to an external torque T, the angular displacement γ is:

$$\gamma = \frac{TD}{2GI_P} \tag{2}$$

Where I_P is the shaft section polar moment of inertia and D its outer diameter. The shaft linear strain ϵ (measured by the strain gauge) is related to the angular displacement γ and the angle respect to the shaft axis α:

$$\epsilon = \frac{\gamma sin(2\alpha)}{2} \tag{3}$$

In order to measure shaft strain, a set of strain gauges (rosette) are placed on the shaft surface to form a Wheatstone bridge circuit [12]. To maximise the measurement resolution, the strain gauge rosette is oriented at a 45 degree angle respect to the shaft axis (see Eq. 3). The actual system used in the sea trials is shown in Fig. 3. The strain gauge rosette (yellowish patch in Fig. 3a) is applied to the shaft using cyanoacrilate glue and wired to the transducer, fixed to the shaft via multiple layers of insulating and glass fiber reinforced tape (see Fig. 3a).

The measurement of the angular speed of the shaft is carried out using a proximity sensor fixed to the boat and a split ring containing 12 equally spaced bolts as seen in Fig.3b . The proximity sensor is then aligned to the bolts hex socket cap in order to ensure a clear output signal.

All the sensors signals are sampled by the acquisition module at 1kHz and later downsampled to 100Hz.

(a) Attaching gauges rosette (b) Completed shaft measurement system

Figure 3. Assembling the onboard shaft measurement system

In addition to the shaft measurements, two Cross Bow CXL04GP3RAL three axis MEMS accelerometers are also sampled. One accelerometer is placed at the yacht's CG, directly over the IMU1 (ACC2, see Fig. 4a). The second accelerometer is placed in the engine room at the base of the generator set (ACC1, see Fig. 4b) .

(a) ACC2 accelerometer at the CG (b) ACC1 accelerometer in the engine room

Figure 4. Accelerometers placement

The propulsion measurements output is a comma separate values ASCII file containing sampled data of time (timecode), shafts rotation frequency and torque together with acceleration values from ACC2.

In order to be able to syncronize the motion database to the propulsion database, ACC2 accelerometer has been placed directly on top of the IMU1. In the post-processing phase, the raw accelerometer signal from the IMU will be compared to the signal from the ACC2 accelerometer and used to compute the delay between the timecodes of the two databases.

3. Results

3.1. Calm Water

In addition to the seakeeping trials, calm water tests have been carried out in order to get a reference for propulsion data. The results refers to two days of testing where the engine rpm was increased by 200 rpm step until full throttle. Propeller shafts rpm and torque measurement are then properly windowed in order to isolate the most appropriate data subset (constant torque and rpm value). The propulsion data is analysed in conjunction with the hull motion data from the on-board IMUs.

Slightly after every acquisition began, the IMU1/ACC2 assembly has been manually knocked three times in order to be able to later recognize the three peaks in raw vertical acceleration. The method of manually align the signals in post-processing using the peaks has been then replaced using the signal cross-correlation technique, that has been proven to be much less time consuming and very accurate, also for calm water results, where vertical motions were very limited.

The plots in Fig. 5 show the calculated shaft torque and power outptut along with the engine limit curves. Data from both starboard (SB) and port side (PS) propeller shafts is plotted, including multiple measurements from the two days of test.Shaft strain has been measured by the strain gauges rosette and torque has been computed using Eqs. (2) and (3), using the young modulus from the ”Acqualoy 17” datasheet provided by the manufacturer and an estimated Poisson ratio at first. Experimental values have then been used, after static tests on a shaft sample have been carried out.

The consistency of the results is very clear from one day to the next, and also the fact that for higher speeds, the starboard shaft always experienced slightly higher torque respect to the port side one. The same is not valid for lower speed where torque values are almost identical (as expected).

The starboard shaft higher torque is due to the fact that the yacht started to heel at higher speed. In particular, positive heel angle is observed in Fig.6b, and according to the IMU reference system, meaning that the yacht is heeled to starboard. This causes the starboard propeller to be more immersed than the port side one resulting in higher loads.

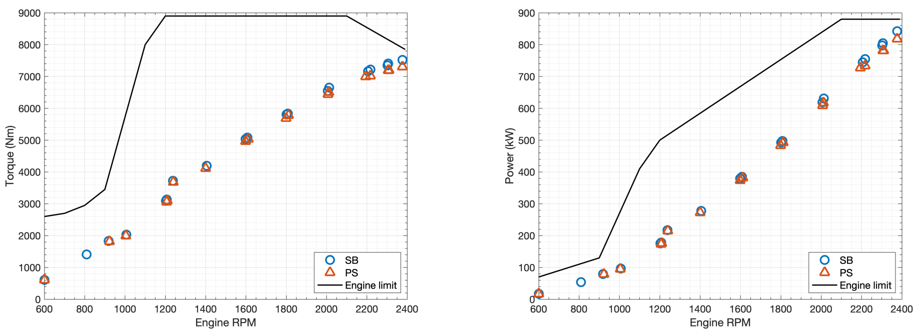

(a) Shaft torque

(b) Power output

Figure 5. Torque and power vs engine rpm

The yacht's trim is plotted in Fig. 6a, along with model data, it is clear that the full scale hull shows higher trim angle respect to the model tests. Comparing the full scale trim to the model at the design loading condition (LC1) it is however clear that the trend with speed is similar, and both show maximum values of trim for the same speed. The main difference between full scale and model scale test condition is that while in the case of model scale tests, the towing force is horizontal and applied near the center of gravity and the case of the yacht thrust is delivered to the lower-placed thrust bearing along the shaft direction. The thrust force in full scale could therefore generate an additional pitching moment and lead to higher running trim values.

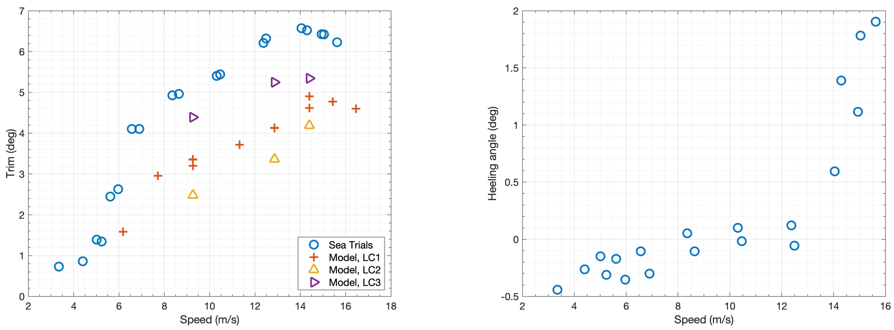

(a) Trim in calm water

(b) Heeling angle

Figure 6. Full-scale trim and heeling angles vs speed

3.2. *Head Sea*

In the the following subsection, some preliminary studies of the effects of the boat motion on the propulsion characteristics measured during seakeeping trials in head seas (χ = 180°) will be presented. The signals of pitch, horizontal accelerations on shaft torque and rpm have been analysed both in the time and frequency domain in order to highlight relevant relationships.

3.2.1. *Frequency Domain Analysis*

The first analysis of the signals has been carried out in the frequency domain, comparing the frequency response of pitch with shaft torque and rpm. This preliminary analysis has been implemented using FFT Fourier transform algorithm to compute the single-sided amplitude spectra of the three signals and then compared. The comparison of normalized pitch, acceleration torque and rps spectra are plotted in Fig. 7, it is clear that all three measurements share a similar frequency response, in particular the peak around the encounter frequency value of 0.4 Hz.

The relationships between hull motions and torque response can be evaluated by means of transfer functions (TF) or response amplitude operator (RAO). Torque RAOs are here defined frequency by frequency and evaluated using wave amplitude (Torque) pitch motion (TorqueP) and horizontal acceleration (TorqueA). As expected, Fig. 7, shows that torque response is better correlated to hull pitch and horizontal acceleration

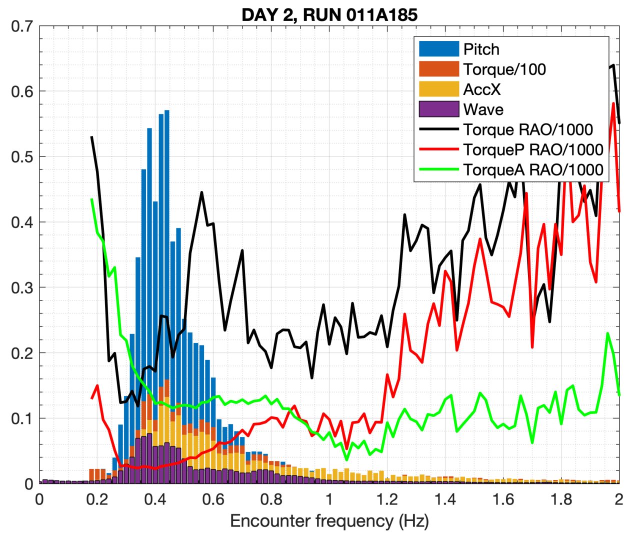

Figure 7. Motion and acceleration spectra along torque RAOs comparison

than to wave amplitude around the response peak, as spectra share similar features and the ratio between them, represented by RAOs, show less variation and flatter trend.

In order to better evaluate the effect of hull motions on shaft torque during 18 knots head sea cruise, all head sea runs torque RAOs have been evaluated by means of the average and standard deviation of RAO values around the peak response frequency interval (0.3-0.8 Hz) in Fig. 8.

Torque RAOs have been evaluated using wave elevation as well as pitch and horizontal acceleration:

$$\mathrm{Torque\,RAO} = \frac{S_{Torque}}{S_{\zeta}}, \quad \mathrm{TorqueP\,RAO} = \frac{S_{Torque}}{S_{Pitch}}, \quad \mathrm{TorqueA\,RAO} = \frac{S_{Torque}}{S_{accX}} \tag{4}$$

Where S_{Torque} is the torque spectra and S_{ζ}, S_{Pitch} and S_{accX} are wave, pitch and horizontal acceleration spectra respectively.

The plots show that in all five runs spread across a month, the average and standard deviation values of the RAOs computed using hull motion measurements show less variation and almost constant average values.

Given the low variation of average torque RAOs across different test runs (see Tab.1), the results obtained shows once more that torque modulation is in fact better related to ship motion response (pitch in particular) instead of directly to the sea state.

The phenomena governing torque fluctuation could be linked to the variation of propeller disk inflow speed due to wave impacts that periodically vary the hull speed, as well to the variation of inflow angle due to the pitching motion. Another possible source could be due to bearing friction modulation due to shaft-propeller precession forces caused by pitching motion.

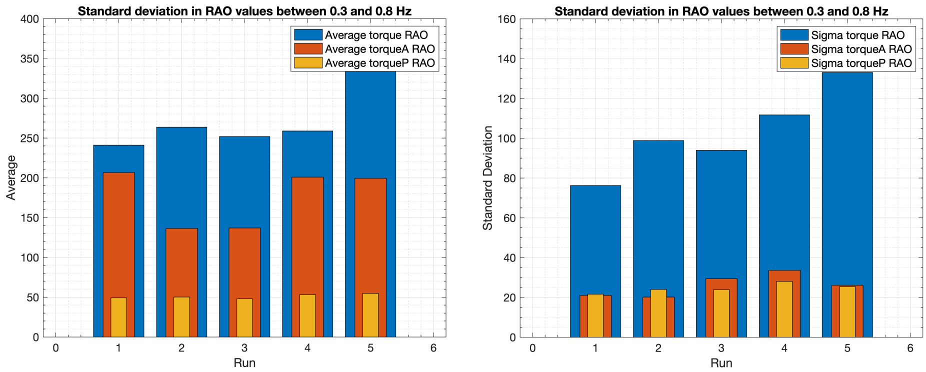

(a) Torque RAOs averages

(b) Torque RAOs standard deviation

Figure 8. Torque RAOs averages and standard deviation comparison

3.2.2. Time Domain Analysis

In this section, the analysis of pitch and horizontal acceleration timeseries together with torque and rpm data is presented in order gain further insight in the relationships between them. In partucular, the methods and results used for assessing phase delay between motions and torque is discussed.

In the case of the time series analysis, the synchronization of the acceleration signals from IMU1 (motions acquisition system) and ACC2 (propulsion acquisition system) at the yachts center of gravity is of paramount importance for later phase analysis. To do so, raw vertical acceleration data from both sensors has been compared and their delay has been computed by means of the cross correlation technique. Once the delay between the two timeseries is found, one of the two datasets (motion or propulsion) is shifted by padding the whole dataset with zeros depending on the sign of the delay. The signals of both motion and propulsion datasets, once synchronized, share the same UTC timestamp, provided by the IMU GNSS system.

The synchronized datasets allow for an analysis of the phase between pitch and the three chosen signals. Since all signals are not monochromatic, an average phase delay has been computed using the signal delay through the application of the cross correlation technique between synchronized pitch and torque signals. Once the time delay is found, the signal's main harmonic frequency has been used to compute the phase angle.

In Fig. 9, example torque timeseries from day two is compared with pitch (Fig. 9a), horizontal acceleration (Fig. 9b) and rotation frequency (Fig. 9c).The plots are normalized and shifted vertically to better compare the signals.

The analysis of pitch and torque timeseries revealed that the torque response has a phase lag of around 120° respect to pitch motion and 90° respect to horizontal acceleration. As expected, the analysis of torque and rps signals revealed that torque and shaft rotation speed are in anti-phase.

In order to have a more significant picture of torque phases in the case of head sea at 18 knots, the phases of four different runs spanning a month are plotted in Fig. 10a. The plot shows that average torque response phases are more or less the same across different tests.

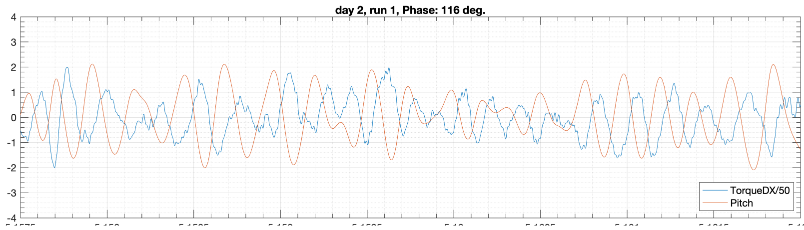

(a)

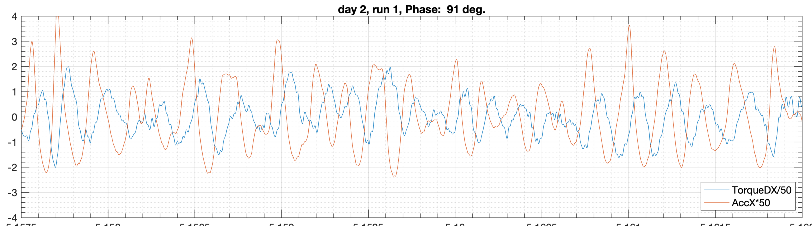

(b)

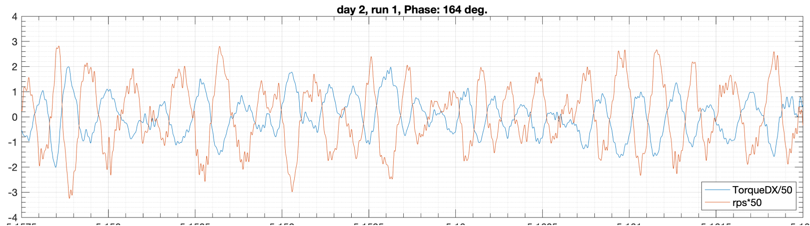

(c)

Figure 9. Pitch, Acceleration and rps timeseries compared to torque response.

The results of the phase analysis show that torque response has a smaller phase lag respect to surging acceleration than pitch and the difference between the two is surprisingly constant across multiple tests (see yellow and blue line in Fig. 10a).

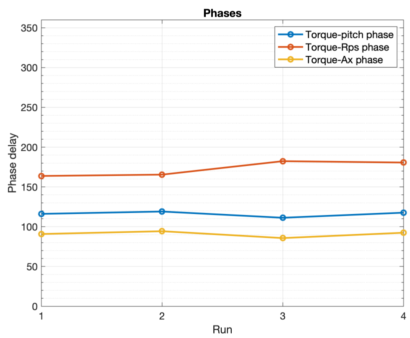

(a) Torque response phases.

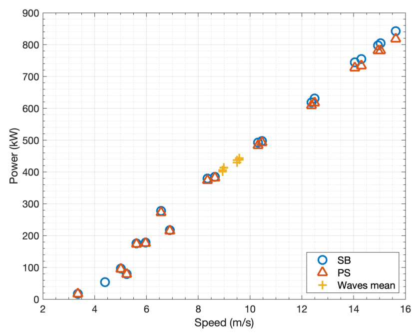

(b) Power output in waves compared to calm water.

In general, it is also worth comparing the effect of mild sea condition on the average power output. As previously shown, the propulsive system is affected when cruising through in head sea. Nonetheless, although the engine response is clearly correlated to the boat motions, average values of power output did not show any significant increase respect to the case of calm water, as it can be easily observed in Fig. 10b (yellow crosses).

3.3. Propeller Shaft Static Test

The evaluation of the propeller shaft shear modulus G (Eq. 1) is one of the most delicate tasks during the measurement of torque values from shaft deformation. The problem lies in the fact that G depends greatly on the composition of the steel with which the shaft is made but unfortunately it is not generally known, since the suppliers measure only the elastic module E.

Even if E and ν values are available, they are often given within a sizable range, thus, in order to have an accurate estimate of the shaft mechanical properties, an experimental approach is needed. The experimental approach consist in a static torsion test on a piece of shaft made with the same material as the one on-board. The experimental setup used to perform the tests is shown in Fig. 10.

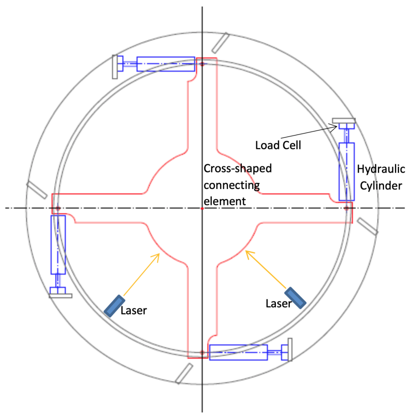

(a) Setup scheme

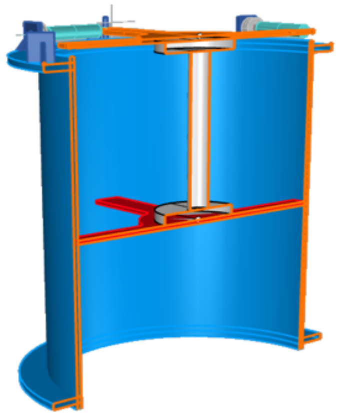

(b) Setup vertical cutaway

Figure 10. Experimental setup top and perspective views.

The lower shaft end is fixed to a large cylindrical structure (in blue in Fig. 10b) with a high torsional rigidity by means of rigid flanges (dark red), the upper end is connected to a cross-shaped rigid element that applies a torque to the shaft by means of four hydraulic cylinders (see Fig. 10a). The force of each cylinder is measured by a load cell in order to accurately measure the applied torque. Two laser transducers are fitted to detect undesired bending of the shaft that may occur if the four cylinder forces are not perfectly equal and tangential. In order to balance the forces of the four cylinder, they are connected to the same hydraulic circuit. The shaft torsional deformation is measured using the same strain gauge rosette make and acquisition system employed during sea trials. Two identical tests have been carried out using nine torque steps in order to obtain reliable average shear modulus values.

The plot in Fig. 11 shows the results of the static tests. The torque meter constant is a function of the shear modulus G and effective torque. It can be noted that unavoidable friction effects in the setup play a noticeably role at low torque. Using data from both measurements outside the range where friction effects are present, the measured shear module G is found to be 75141 Nm/mm2 with 0.3%.

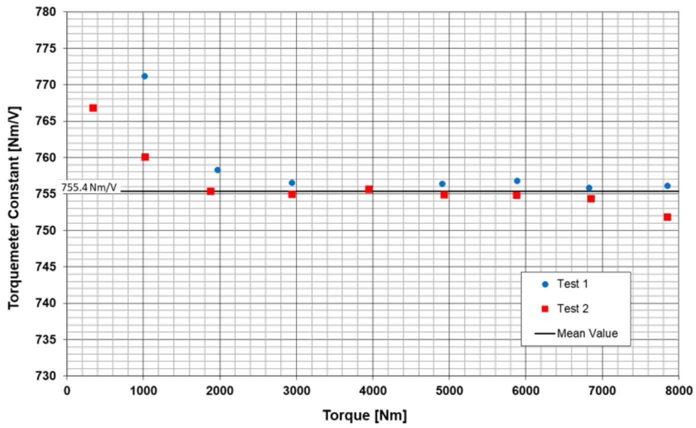

Figure 11. Results of static torque tests.

4. Conclusions

In this paper, a comprehensive description of the experimental setup and analysis of full scale seakeeping trials propulsion data of a 65 ft planing pleasure yacht is presented. Torque and rpm have been measured on both propeller shafts during seakeeping trials in mild sea conditions, along with hull motions and accelerations. Both calm water and seakeeping experiments have been carried out and their setup and results have been presented. Calm water results have been compared with towing tank tests and engine limit curves, and provided a baseline for seakeeping results in terms of power output.

Seakeeping data analysis of both motion and propulsive system sensors has been carried out in both frequency and time domain, uncovering some relationships between motions and torque response. Torque response amplitude operators (RAOs), computed using wave, horizontal acceleration and pitch amplitude have been compared. It is found that torque is better correlated to hull motions than to wave excitation, average torque RAOs of multiple tests show that their value is reasonably constant for the case of mild head sea conditions at 18 knots. In order to provide an in-depth look at the effects of rough weather on the propulsion system, torque timeseries have been also analyzed along with pitch, horizontal acceleration and rotation frequency. Average torque response phase lag respect to motions has shown that phase values are reasonably constant during multiple tests and in particular it is observed that torque phase lag respect to acceleration is less than the one respect to pitching motion.

Tests on a shaft sample have been carried out in order to validate its mechanical properties and hence quantitative results regarding shaft torque.

A detailed analysis of the propulsion system response of a planing pleasure yacht in mild weather conditions is shown. The main novelty lays in both frequency and time domain analysis of the torque response, along with the experimental assessment of the mechanical properties of the propeller shaft. In particular, torque RAOs and phases have been characterized and show good consistency across mulitple test runs. Future work will include a comparison of calm water results with model self propulsion tests and simulations.

References

[1] Allen RG, Jones RR, Taylor DW. A simplified method for determining structural design-limit pressures on high performance marine vehicles. In: Advanced Marine Vehicles Conference 1978 Apr (p. 754).

[2] Kallio JA. Results of Full Scale Trials on Two High Speed Planing Craft (KUDU 2 and KAAMA). DAVID W TAYLOR NAVAL SHIP RESEARCH AND DEVELOPMENT CENTER BETHESDA MD SHIP PERFORMANCE DEPT; 1978 Jul.

[3] J Ooms and Jan Alexander Keuning. Comparative full scale trials of two fast rescue vessels. In: TUDelft, Faculty of Marine Technology, Ship Hydromechanics Laboratory Report 1100-P, International Conference SURV IV, Surveillance, Pilot & Rescue Craft for the 21st Century, Gothenburg, Sweden. 1997.

[4] Richard H Akers et al. Predicted vs. measured vertical-plane dynamics of a planing boat. In: FAST. Vol. 99. 1999, pp. 91105.

[5] Karl Garme and Anders Rosn. Time-domain simulations and full-scale trials on planing craft in waves. In: International Shipbuilding Progress 50.3 (2003), pp. 177 208.

[6] Hans Jorgen B Mørch and Ole A Hermundstad. Planing craft in waves-Full scale measurements. In: Proceedings of the International Conference on Fast Sea Transportation, FAST2005, June 2005, St. Petersburg, Russia, Paper: P2005-2 Proceedings. 2005.

[7] JA Keuning, F Van Walree, et al. The comparison of the hydrodynamic behaviour of three fast patrol boats with special hull geometries. In: HIPER 06: 5th International Conference on High-performance Marine Vehicles. Australian Maritime College. 2006, p. 137.

[8] NC Townsend, PA Wilson, and S Austen. What influences rigid inflatable boat motions? In: Proceedings of the Institution of Mechanical Engineers, Part M: Journal of Engineering for the Maritime Environment 222.4 (2008), pp. 207217.

[9] Puzzer, T., Pigazzini, R., Davison, S., Morgut, M., & Contento, G. (2019, July). Full-Scale Seakeeping Trials: An Integrated Analysis of Sea State and On-board Data. In The 29th International Ocean and Polar Engineering Conference. International Society of Offshore and Polar Engineers.

[10] F Prini et al. Full-Scale Seakeeping Trials of an All-Weather Lifeboat. In: SURV 9 Conference: Surveillance, Pilot & Rescue Craft, London, UK: The Royal Institution of Naval Architects. 2018.

[11] Josef Camilleri, DJ Taunton, and Pandeli Temarel. Full-scale measurements of slamming loads and responses on high-speed planing craft in waves. In: Journal of Fluids and Structures 81 (2018), pp. 201229.

[12] Carlton, John. Marine propellers and propulsion. Butterworth-Heinemann, 2018.

[13] van Deyzen, A. F. J., Keuning, J. A., & Huijsmans, R. H. M. (2012). Smart control of fast shipsPart 1: A setup for automated proactive control of the thrust used to increase the operability of a small planing monohull sailing in head seas. International shipbuilding progress, 59(1-2), 1-19.

[14] van Deyzen, A. F. J., Keuning, J. A., & Huijsmans, R. H. M. (2012). Smart control of fast shipsPart 2: A conceptual model of automated proactive thrust control. International shipbuilding progress, 59(1-2), 21-54.